



In Vivo Dissection of the Intrinsically Disordered Receptor Domain of Tim23

Umüt Günsel¹, Eyal Paz², Ruhita Gupta¹, Isabella Mathes³, Abdussalam Azem² and Dejana Mokranjac¹

1 - BMC-Physiological Chemistry, LMU Munich, 82152 Martinsried, Germany

2 - Department of Biochemistry and Molecular Biology, The George S. Wise Faculty of Life Sciences, Tel Aviv University, Tel Aviv 69978, Israel

3 - MPI of Biochemistry, 82152 Martinsried, Germany

Correspondence to Dejana Mokranjac: BMC-Physiological Chemistry, LMU Munich, Großhadernerstr. 9, 82152 Martinsried, Germany. dejana.mokranjac@bmc.med.lmu.de

<https://doi.org/10.1016/j.jmb.2020.03.031>

Edited by Ichio Shimada

Abstract

In the intermembrane space (IMS) of mitochondria, the receptor domain of Tim23 has an essential role during translocation of hundreds of different proteins from the cytosol *via* the TOM and TIM23 complexes in the outer and inner membranes, respectively. This intrinsically disordered domain, which can even extend into the cytosol, was shown, mostly *in vitro*, to interact with several subunits of the TOM and TIM23 complexes. To obtain molecular understanding of this organizational hub in the IMS, we dissected the IMS domain of Tim23 *in vivo*. We show that the interaction surface of Tim23 with Tim50 is larger than previously thought and reveal an unexpected interaction of Tim23 with Pam17 in the IMS, impairment of which influences their interaction in the matrix. Furthermore, mutations of two conserved negatively charged residues of Tim23, close to the inner membrane, prevented dimerization of Tim23. The same mutations increased exposure of Tim23 on the mitochondrial surface, whereas dissipation of membrane potential decreased it. Our results reveal an intricate network of Tim23 interactions in the IMS, whose influence is transduced across two mitochondrial membranes, ensuring efficient translocation of proteins into mitochondria.

© 2020 The Author(s). Published by Elsevier Ltd. This is an open access article under the CC BY-NC-ND license (<http://creativecommons.org/licenses/by-nc-nd/4.0/>).

Introduction

Many intrinsically disordered proteins occupy key positions in cellular signaling networks due to their ability to interact with different proteins leading to different cellular outcomes [1]. In the intermembrane space (IMS) of mitochondria, the intrinsically disordered domain of Tim23 has an essential role in biogenesis of mitochondria and was shown to interact with a number of partner proteins. During biogenesis of mitochondria, hundreds of different mitochondrial precursor proteins with N-terminal presequences are translocated from the cytosol to the final place of their function within the organelle with the help of the TOM and TIM23 complexes in the outer and inner membranes, respectively [2–9]. After initial translocat-

tion across the TOM complex, presequences are recognized by the IMS-exposed receptors of the TIM23 complex. In a membrane potential dependent manner, presequences are then delivered to the membrane-embedded translocation channel of the TIM23 complex. Finally, complete translocation of the polypeptide chain across the inner membrane is mediated by ATP-dependent action of the matrix-exposed import motor of the TIM23 complex. If the translocating protein contains an additional lateral sorting signal downstream of the presequence, translocation into the matrix will be stalled and the TIM23 complex will open laterally to insert the hydrophobic segment into the inner membrane.

Tim23 is the central, name-giving component of the TIM23 complex. It contains an N-terminal *ca.*

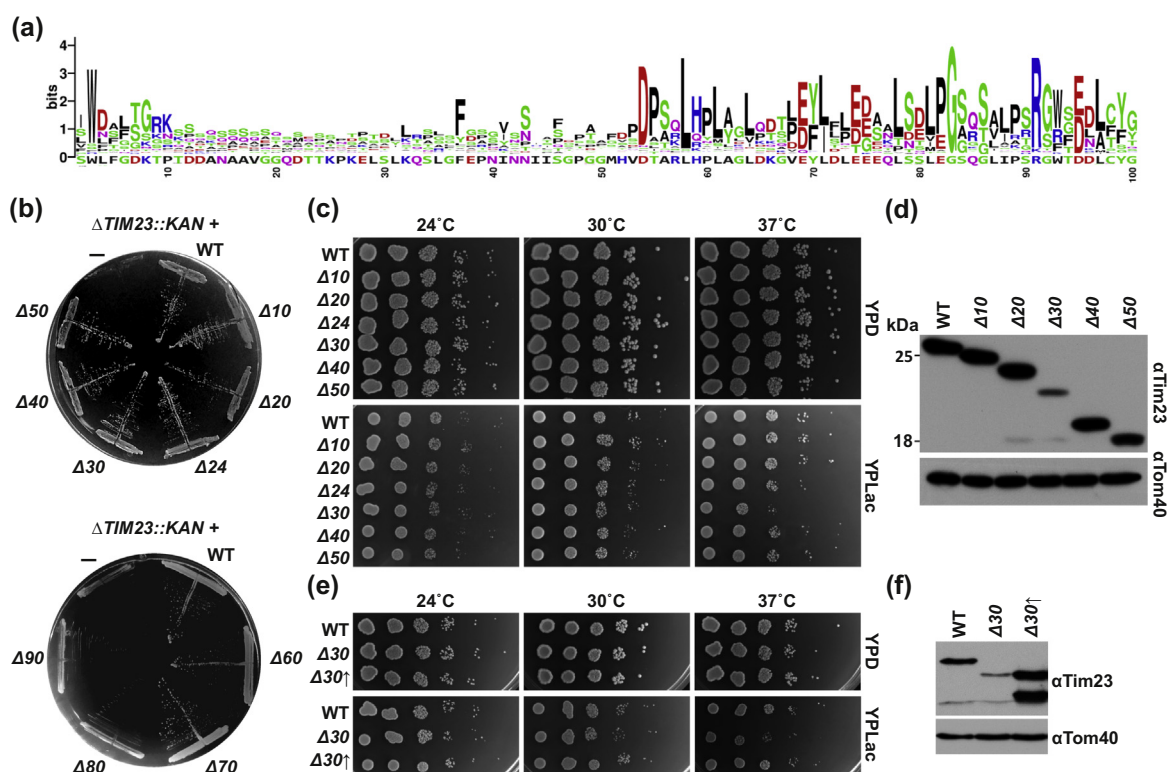


Figure 1. Deletion of the first 70 residues of Tim23 can be tolerated by yeast cells. (a) Sequence conservation of the IMS segment of Tim23 based on 795 identified sequences. (b) The ability of N-terminal truncation mutants of Tim23 to support the function of the full-length protein was analyzed on plates containing 5-FOA. Empty vector and a vector encoding the WT version of Tim23 were used as negative and positive controls, respectively. (c and e) Growth of the indicated Tim23 truncation mutants was analyzed by serial dilution spot assay on plates containing a fermentable- (YPD) or nonfermentable- (YPLac) carbon source at indicated temperatures. (d and f) Isolated mitochondria (d) and total cell extracts (f) of the indicated mutants were analyzed by SDS-PAGE and immunoblotting with Tim23 antibody. Tom40 was used as control.

100-amino-acid-residue-long segment in the IMS and a C-terminal segment of a similar length in the inner membrane. The latter segment contains four predicted transmembrane helices that form, likely together with Tim17, the translocation channel of the TIM23 complex [10–16]. Together with Tim50, the IMS-exposed domain of Tim23 serves as the receptor of the TIM23 complex [17–26]. Point mutations in Tim23 and in Tim50 that destabilize the interaction of the two proteins in the IMS prevent transfer of precursor proteins from TOM to TIM23 complex, impairing translocation of proteins along the presequence pathway and leading to cell death [25,27,28]. The first *ca.* 20 residues of Tim23 are exposed to the cytosolic surface of mitochondria [29], bringing TOM and TIM23 complexes closer together and thereby facilitating protein import into mitochondria. This accessibility of Tim23 in intact mitochondria to externally added proteases is a dynamic process and it depends not only on Tim23 interaction with Tim50 [25,26,28] but also on the translocation activity of the TIM23 complex [30] and on the integrity of the TOM complex [31].

Besides interacting with Tim50 and presequences, the IMS domain of Tim23 was also found to interact with Tim21 [20,32], a nonessential subunit of the TIM23 complex, Tom22 [25,32], a subunit of the TOM complex, and to be involved in homodimerization of Tim23 [17,33]. Intriguingly, the vast majority of these various interactions were analyzed only *in vitro*, using recombinantly expressed IMS domain of Tim23 that is largely, if not completely, unfolded [28,34]. Here, we comprehensively dissected the IMS domain of Tim23 *in vivo*.

Results and Discussion

Deletion of first 70 residues of Tim23 can be tolerated by yeast cells

Sequence analysis of the predicted IMS-exposed regions of 795 Tim23 proteins [35] shows rather poorly conserved first *ca.* 50 residues and a higher sequence conservation in the second half of the IMS domain

(Figure 1(a)), in agreement with previous findings showing that the deletion of the first 50 residues of Tim23 can be tolerated by yeast cells but that the removal of the entire IMS domain is lethal [17,18,31]. To dissect the IMS domain of Tim23 more systematically *in vivo*, we truncated the protein by 10 residues at the time and analyzed the ability of the shortened versions to support the function of the full-length protein. Yeast cells expressing Tim23 versions lacking up to 70 residues from the N terminus were viable (Figure 1(b)). Deletion of 80 or 90 residues from the N terminus cannot be tolerated by yeast cells. We analyzed growth of mutants lacking up to 50 residues in more detail. On a fermentable carbon source, we observed no obvious growth defect for any of the truncation mutants (Figure 1(c)). On a nonfermentable carbon source, cells expressing Tim23 lacking the first 30 residues showed an obvious growth defect at 37 °C. Analysis of mitochondria isolated from cells expressing truncated versions of Tim23 showed severely reduced levels of Tim23Δ30 (Figure 1(d)), compared to the other truncations, raising the possibility that the observed phenotype may be due to lower Tim23 levels. Indeed, growth of yeast cells was largely recovered upon overexpression of Tim23Δ30 (Figure 1(e) and (f)). Though the deletion of the first 10 residues of Tim23 showed no obvious growth defect, this region was previously implicated in Tim21 and Tim50 binding when recombinant proteins were analyzed [32]. To analyze whether this region of Tim23 plays a critical role in binding to Tim21 and Tim50 *in vivo*, we performed coimmunoprecipitations from mitochondria isolated from cells expressing wild-type (WT) or Tim23Δ10 (Sup. Figure 1). The coimmunoprecipitation profiles of the two types of mitochondria were essentially indistinguishable, demonstrating that the first 10 residues of Tim23 may contribute to but are not essential *in vivo* for either Tim50 or Tim21 binding.

Tim23–Tim50 interaction surface is larger than previously shown

As the sequence conservation after residue 50 of Tim23 increases, we analyzed the rest of the IMS domain of Tim23 by alanine scanning mutagenesis. In the region between residues 51 and 85, consecutive residues of Tim23 were mutated to alanines and the growth of the obtained mutants was analyzed on both fermentable and nonfermentable carbon sources (Figure 2(a)). Only one mutant, 68A5, showed a very strong growth defect. The version of Tim23 in which residues 68 to 72 are mutated to alanines was growing poorly on glucose-containing medium at both 24 and 30 °C and not at all at 37 °C. On a nonfermentable carbon source, this mutant was essentially inviable. We made similar observation when the five residues were mutated to glycines and saw somewhat weaker, but

still obvious, growth defect when 68 N5 mutant was analyzed (Sup. Figure 2a). This region contains two conserved residues, Y70 and L71, which were previously shown to be involved in the interaction with Tim50 both *in vivo* and *in vitro* [21,25,28]. However, the growth phenotype of Y70A/L71A double mutant is far milder than that of the 68A5 mutant. Sequence analysis of this region showed a high conservation also of the residue E69. To dissect the importance of individual residues in this region, we made a E69A single mutant and a triple mutant in which all three conserved residues, 69, 70, and 71, are mutated to alanines, E69A3. E69A mutant grew like WT on all media and temperatures analyzed, similar to the previously described Y70A and L71A single mutants (Figure 2(b)). E69A3 was, however, growing worse than Y70A/L71A double mutant, in particular on a nonfermentable carbon source. Still, it grew better than the 68A5 mutant. This suggests that the observed phenotype of the 68A5 mutant is cumulative, with contributions of all five residues. The contribution of the residues V68 and D72 appears though to be the smallest as the respective single mutants as well as the double mutant showed no obvious growth defect at any of the temperatures analyzed (Figure 2(b)). This is also in agreement with their weaker conservation. To further genetically dissect the role of residue E69, we combined E69A mutation with either Y70A or L71A mutations in E69A/Y70A and E69A/L71A double mutants. E69A/L71A double mutant grew worse than the single mutants, but still better than the previously analyzed Y70A/L71A double mutant (Figure 2(c)). E69A/Y70A double mutant showed no obvious growth defect. We conclude that the stretch between residues 68 and 72 contains, in addition to previously identified Y70 and L71, further functionally important residues, in particular E69. Residue L71 seems to be the most important in this stretch, though clearly all five residues contribute to the observed phenotype.

What is the role of E69? We isolated mitochondria from E69 mutant cells and performed coimmunoprecipitation experiment from digitonin-solubilized mitochondria. The interaction between Tim50 and Tim23 was impaired in the E69A mutant as seen by both reduced coprecipitation of Tim50 with Tim23 antibodies as well as by reduced coprecipitation of Tim17 and Tim23 with antibodies to Tim50 (Figure 2(d)). Interestingly, E69A mutation reduced, but did not abolish, Tim23–Tim50 interaction. In contrast, in L71A single mutant and in Y70A/L71A double mutant, Tim23–Tim50 interaction was essentially absent. Though in previous NMR studies this stretch of Tim23 was also identified as important for interaction between Tim23 and Tim21 [32], we observed no difference in Tim21 recruitment to Tim23 *in organello* in any of the mutants analyzed (Figure 2(d)). We conclude that, in addition to Y70

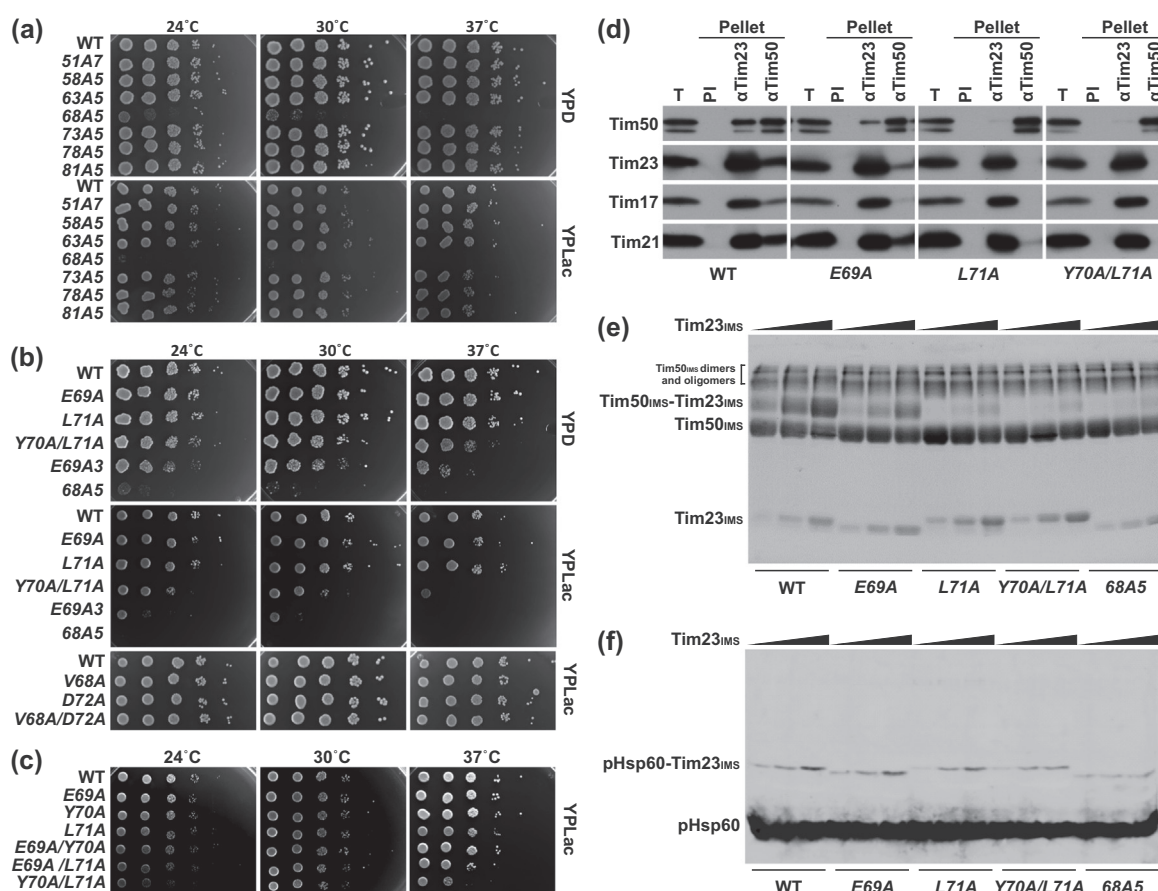


Figure 2. Tim50 binding region on Tim23 is larger than previously identified. (a) Consecutive residues of Tim23 in the region between residues 51 to 85 were mutated to alanines, and the growth of the obtained yeast strains was analyzed by serial dilution spot assay as described in Figure 1(c). Explanation for the nomenclature used - the number in front of A indicates the first residue that was mutated to an alanine and the number behind indicates how many consecutive residues were mutated to alanines. (b and c) Indicated mutants were analyzed by serial dilution spot assay as described in Figure 1(c). (d) Mitochondria isolated from WT and the indicated mutant cells were solubilized with 1% digitonin and subjected to immunoprecipitation with affinity purified antibodies against Tim23 and Tim50. Antibodies from preimmune serum (PI) were used as a negative control. Samples were analyzed by SDS-PAGE and immunoblotting with indicated antibodies. Total (T): 20% and pellets: 100%. (e) Recombinant Tim50_{IMS} (10 μ M) was mixed with increasing amounts of the indicated versions of recombinant Tim23_{IMS} (5, 10, and 20 μ M) and incubated with an amino group-specific crosslinker disuccinimidyl suberate (1 mM). Samples were analyzed by SDS-PAGE and Coomassie Brilliant Blue staining. (f) Biotin-labeled pHsp60 peptide (2 μ M) was mixed with increasing amounts of the indicated versions of recombinant Tim23_{IMS} (10, 20, and 30 μ M) and incubated with an amino group specific crosslinker disuccinimidyl suberate (50 μ M). Samples were analyzed by SDS-PAGE followed by immunoblotting with Streptavidin Alexa Fluor 680 conjugate.

and L71, residue E69 is also involved in the interaction between Tim23 and Tim50.

To further confirm that E69 has a direct role in Tim23–Tim50 interaction, we turned to a previously established *in vitro* system [28] in which we can directly analyze Tim23–Tim50 interaction without potentially contributing effects of other components of the TIM23 complex present in mitochondria. When recombinantly expressed and purified IMS domains of Tim23 and Tim50 are incubated together in the presence of an amino group-specific crosslinker DSS, a Tim23_{IMS}–Tim50_{IMS} crosslinking adduct is

observed (Figure 2(e) and Sup. Figure 2b). This adduct is essentially lost when the versions of Tim23 containing L71A mutation, either alone or in combination with other residues in the 68–72 stretch, were used. When we analyzed Tim23E69A, the Tim23_{IMS}–Tim50_{IMS} crosslinking was reduced but not abolished. Thus, this *in vitro* experiment fully supports the *in organello* findings.

Is the stretch between residues 68 and 72 also involved in binding of Tim23 to presequences? Considering the positively charged nature of presequences, negatively charged E69 seemed

in this respect particularly interesting. Biotinylated presequence peptide of Hsp60 can be crosslinked to the recombinantly expressed and purified Tim23_{IMS} [36]. We observed essentially no reduction in crosslinking efficiency of the Tim23E69A mutant compared to WT and rather minor reduction with L71A and Y70A/L71A mutants (Figure 2(f)). Even the 68A5 mutation did not completely abolish the interaction of Tim23_{IMS} with the Hsp60 presequence peptide. The previous work identified L71 as the residue with the largest chemical shift changes upon incubation of Tim23_{IMS} with peptides corresponding to presequences of ALDH and COXIV [34]. It is possible that the presequence of Hsp60 may be recognized in a different way compared to ALDH- and COXIV presequences. However, it is also possible that multiple regions of Tim23_{IMS} contribute to binding of presequences [34]. Still, the reduced interaction seen with the 68A5 mutant suggests that Tim23 binds presequences and Tim50 in at least partially functionally overlapping manner.

Besides the interaction site for Tim50, the region between residues 51 and 85 of Tim23 also contains a region (amino acid residues 58 to 61) that was previously implicated in Tim23 interaction with Tom22 [32]. Though the alanine scanning mutagenesis did not reveal any obvious growth defect of the 58A5 mutant (Figure 2(a)), we reasoned that the multiplicity of TOM–TIM23 interactions *in vivo* [31] may mask the Tim23–Tom22 interaction identified by NMR. Tim23–Tom22 interaction was previously observed *in vivo* using site-specific UV crosslinking with a photoactivatable unnatural amino acid p-benzoyl-phenylalanine (Bpa) introduced at position 41 of Tim23 [25]. We introduced Bpa at 11 positions within the first 40 residues of Tim23, exposed the cells to UV light and looked for Tim23–Tom22 crosslinks. Only when Bpa was introduced at positions 37 and 40, we observed a UV-specific crosslink between Tom22 and Tim23 (Sup. Figure 2c). This shows that the Tim23 interaction surface with Tom22 is found more to the middle of the IMS domain of Tim23, rather than at its very beginning, at least under conditions of no translocation. To analyze the influence of the region between residues 58 and 61 of Tim23 on the interaction with Tom22, we combined Bpa at position 40 with 58A5 mutation. The crosslink between Tim23 and Tom22 was largely retained in this mutant (Sup. Figure 2d), suggesting that residues 58 to 61 may not be the major interaction site between Tom22 and Tim23. Interestingly, when we combined Bpa at position 40 with the Y70A/L71A mutation, we also observed no major effect on Tim23–Tom22 crosslinking. Even though the same mutation abolishes Tim23–Tim50 interaction and completely prevents exposure of Tim23 on the mitochondrial surface [25,28], Tim23 can apparently still interact with Tom22 in the IMS.

Mutagenesis analysis of the very C-terminal segment of the IMS domain of Tim23 reveals an interaction site for Pam17

Alanine-scanning mutagenesis of the very C-terminal region of the IMS domain of Tim23 revealed several partly overlapping mutants that impaired growth of yeast cells, most prominently on a nonfermentable carbon source and at an elevated temperature (Figure 3(a)). We first analyzed 87A5 mutant which grew slower than WT at 37 °C both on glucose- and on lactate-containing medium. The same was observed when, instead of alanines, mutations to glycine or asparagine residues were made (Sup. Figure 3). This region of the IMS domain of Tim23 has not been previously implicated in any of the interactions. The protein profiles of isolated mitochondria revealed no obvious difference in endogenous levels of any of the TIM23 subunits or control mitochondrial proteins analyzed (Figure 3(b)), suggesting that the impaired expression or stability of Tim23 are not the reason behind the growth defect. We did, however, observe an altered running behavior of Tim23 upon SDS-PAGE in this mutant. To understand the molecular basis of the observed impaired growth, we analyzed the ability of isolated mitochondria to import precursor proteins. Several artificial and endogenous substrates of the TIM23 complex were imported with reduced efficiency in 87A5 mitochondria, compared to WT (Figure 3(c)). The defect was observed irrespective whether we analyzed translocation into the matrix ($b_2(1-167)\Delta$ DHFR, F1 β , and Tim44) or lateral insertion into the inner mitochondrial membrane (DLD and $b_2(1-167)$ DHFR) by the TIM23 complex. In contrast, precursor of the ATP/ADP carrier, whose import does not depend on the TIM23 complex, was imported in 87A5 mitochondria with efficiency indistinguishable from WT. In agreement with this latter finding, 87A5 mitochondria had essentially the same membrane potential as WT (Figure 3(d)). We note that imports of $b_2(1-167)\Delta$ DHFR and F1 β were affected more than import of Tim44 into 87A5 mitochondria. Interestingly, $b_2(1-167)\Delta$ DHFR and F1 β were recently shown to belong to the group of hypersensitive precursors, import of which is particularly dependent on the presence of Pam17, a nonessential subunit of the TIM23 complex with a modulatory role during translocation of proteins [30,37,38], and its interplay with Tim50 [37]. Tim44 does not belong to this group, and its import was also affected to a lesser degree in 87A5 mutant mitochondria.

Crosslinking of Tim23 in intact mitochondria is a sensitive indicator of the state of the TIM23 complex [30]. To analyze whether the 87A5 mutation affects the molecular environment of Tim23, we compared the crosslinking pattern of Tim23 in WT and 87A5 mutant mitochondria

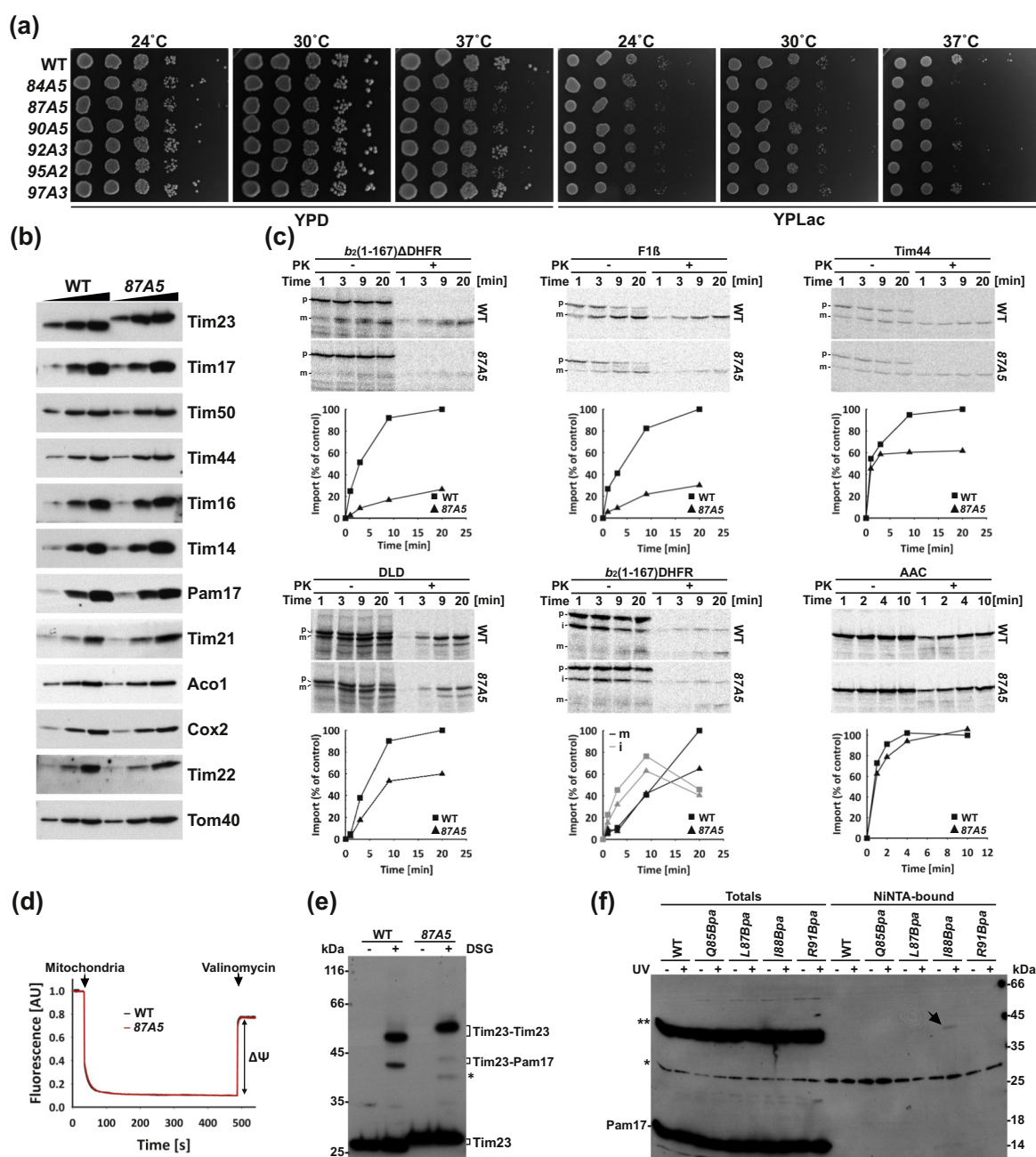


Figure 3. Identification of Tim23–Pam17 interaction site in the IMS. (a) Indicated alanine mutants of Tim23 were analyzed by serial dilution spot assay as described in Figure 1(c). Nomenclature of the mutants was as described in Figure 2(a). (b) Isolated mitochondria (10, 20, and 40 μ g) were analyzed by SDS-PAGE followed by immunoblotting with the depicted antibodies. (c) Indicated mitochondrial precursor proteins were synthesized in the presence of 35 S-methionine and imported into isolated mitochondria. At indicated time points, aliquots were removed and one-half was treated with proteinase K (PK) to remove non-imported material. Mitochondria were reisolated and samples analyzed by SDS-PAGE and autoradiography (upper panels). Quantifications of the import reactions are shown in the lower panels. The amount of PK-protected mature form in the longest time point in WT mitochondria was set to 100%. Precursor (p), intermediate (i), and mature (m) forms of imported proteins. (d) Membrane potential of isolated mitochondria was measured using DiSC₃(5). (e) Isolated mitochondria were treated with an amino group-specific crosslinker disuccinimidyl glutarate (DSG). After quenching of the crosslinker, samples were analyzed by SDS-PAGE and immunoblotting with an antibody against Tim23. *Unidentified crosslinking product of Tim23. (f) Cells expressing C-terminally His-tagged Tim23 with Bpa introduced at the indicated positions were exposed to UV irradiation, where indicated. Total cell extracts were prepared under denaturing conditions, and Tim23-His and its crosslinking products were enriched by binding to NiNTA-Agarose beads. Samples were analyzed by SDS-PAGE and immunoblotting with an antibody against Pam17. * and ** indicate nonspecific bands, and the arrow indicates the crosslink between Tim23 and Pam17.

(Figure 3(e)). In WT, Tim23 gives two prominent crosslinks: a crosslinked Tim23 dimer and a crosslink to Pam17 [30]. In 87A5 mutant mitochondria, crosslinked Tim23 dimers were present as in WT. In contrast, the crosslink to Pam17 was severely reduced and a novel crosslink to a currently unknown protein of ca. 15 kDa appeared. The reduced crosslinking efficiency between Tim23 and Pam17 is in line with the above described differences in import efficiencies among the matrix targeted precursors in 87A5 mitochondria. This result thus implicates also Tim23 in the interplay between Pam17 and Tim50 during import of hypersensitive precursors. The reduced crosslinking efficiency between Tim23 and Pam17 is, however, particularly interesting as crosslinking between Pam17 and Tim23 occurs in the matrix (Pam17 has no lysine residues exposed to the IMS [38]), suggesting that the effects of the mutations in the IMS are transduced through the IM into the matrix. To check whether Tim23 interacts with Pam17 also in the IMS, we introduced Bpa at several positions in the region around residue 87. Indeed, a UV-specific crosslink between Tim23 and Pam17 was identified when Bpa was introduced at position 88 in Tim23 (Figure 3(f)). This shows that Tim23 and Pam17 also interact with each other in the IMS and that the impairment of this interaction can be sensed on the other side of the IM in the matrix.

Two conserved negative charges at the border with the IM affect dimerization of Tim23

The second mutant in the C-terminal region of the IMS domain of Tim23 we analyzed is 95A2. Neutralization of the two conserved negative charges at positions 95 and 96 to alanines resulted in a slower growth at elevated temperatures on both fermentable and nonfermentable carbon sources (Figure 3(a)). Reversal of the charges in the 95 K2 mutant resulted in an even stronger growth defect (Figure 4(a)). Mitochondrial protein profiles showed that neither of the double mutants affected endogenous levels of any of the TIM23 subunits or any other mitochondrial protein analyzed (Figure 4(b)). Still, the ability of isolated mutant mitochondria to import proteins *via* the TIM23 complex, both into the matrix and into the inner membrane, was reduced, whereas TIM23-independent import was unaffected (Figure 4(c)). The membrane potential of the mutant mitochondria was marginally, if at all, reduced (Figure 4(d)).

What is the reason behind the impaired ability of TIM23 to import presequence-containing proteins? The crosslinking experiment, as described above for the 87A5 mutant, revealed that the crosslink to Pam17 was not dramatically reduced in 95A2 and 95 K2 mutants (Figure 4(e)). In contrast, the crosslinked Tim23 dimers were reduced in 95A2 mutant

and essentially absent in 95 K2. This suggests that the dimerization of Tim23 is influenced by residues that are very close to the IM. Is dimerization of Tim23 also affecting its exposure on the mitochondrial surface? Tim23 is accessible to externally added protease in intact mitochondria generating a clipped fragment [25,29,30]. In 95 K2 mutant, the clipped fragment was generated faster than in WT (Figure 4(f)), suggesting that dimerization of Tim23 and its exposure on the surface of mitochondria may be in a dynamic balance.

Exposure of Tim23 on the surface of mitochondria is influenced by membrane potential

We determined the position where proteinase K cuts Tim23 in intact mitochondria. To do so, we treated intact mitochondria isolated from cells expressing a C-terminally His-tagged version of Tim23 with proteinase K, stopped the protease, solubilized mitochondria in SDS-containing buffer, and incubated mitochondrial lysate with NiNTA-Agarose beads. Specifically bound proteins were separated by SDS-PAGE and blotted onto a PVDF membrane. Bands corresponding to full-length and clipped forms of Tim23 were then subjected to automated Edman degradation. No signal was detected for full-length protein, suggesting that the N-terminal amino group of Tim23 is modified. For the clipped form, we detected the following sequence: VGGQDTTKP (Figure 5(a)), showing that proteinase K cuts Tim23 in intact mitochondria after residue 17.

In the end, we analyzed whether membrane potential across inner mitochondrial membrane also influences exposure of Tim23 on the mitochondrial surface. We energized WT mitochondria or dissipated their membrane potential before treatment with proteinase K. Dissipation of membrane potential slowed down the kinetics of Tim23 clipping (Figure 5(b)), suggesting that the events at the inner mitochondrial membrane can be transduced all the way to the cytosolic surface of mitochondria.

Conclusions

Here, we have functionally dissected the IMS domain of Tim23. Our data revealed an intricate network of Tim23 interactions in the IMS whose effects are, intriguingly, transduced across both mitochondrial membranes.

Novel insights into Tim23 interactions with Tim50 and Tom22 suggest that they are relatively independent of each other, supporting the notion that TOM-TIM23 cooperation is ensured by several, partially redundant contacts [18,25,31,39]. The particularly interesting feature of the TOM-TIM23 cooperation is the very N-terminal segment of Tim23, which

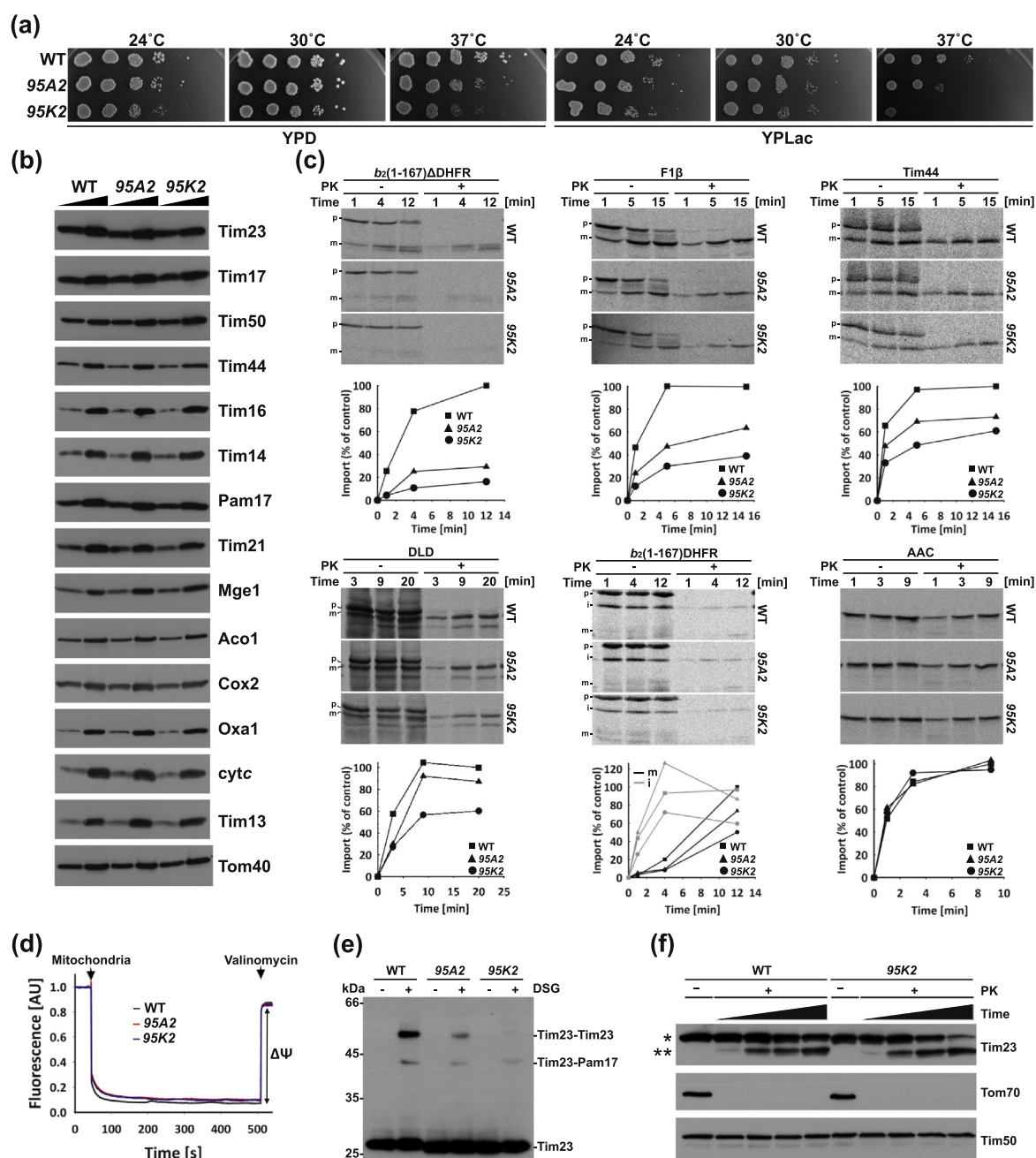


Figure 4. Two conserved negatively charged residues at positions 95 and 96 affect dimerization of Tim23 and its exposure on the mitochondrial surface. (a) Indicated yeast strains were analyzed by serial dilution spot assay as described in Figure 1(c). (b) Isolated mitochondria (10 and 25 μ g) were analyzed by SDS-PAGE followed by immunoblotting with the depicted antibodies. (c) *In vitro* import of 35 S-labeled precursor proteins into isolated mitochondria was performed and analyzed as described in Figure 3(c). Precursor (p), intermediate (i), and mature (m) forms of imported proteins. (d) Membrane potentials were measured using DiSC₃(5). (e) Isolated mitochondria were treated with disuccinimidyl glutarate (DSG). After quenching of the crosslinker, samples were analyzed by SDS-PAGE and immunoblotting with an antibody against Tim23. (f) Isolated mitochondria were incubated with proteinase K (PK), where indicated. After 2, 10, 20, and 40 min, samples were removed and the protease digestion was stopped. Mitochondria were reisolated and the samples analyzed by SDS-PAGE and immunoblotting. Tom70 and Tim50 were used as markers for outer and inner membrane proteins, respectively. *Full-length and **clipped versions of Tim23.

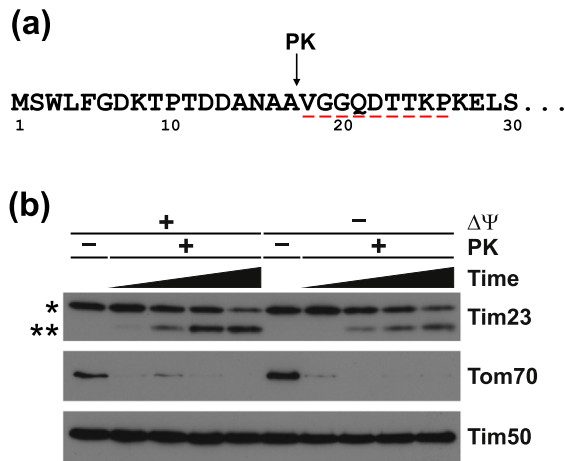


Figure 5. Membrane potential modulates exposure of Tim23 on the mitochondrial surface. (a) The site of Tim23 accessible to proteinase K (PK) in intact mitochondria was determined by automated Edman degradation. Amino acids identified by Edman degradation of the clipped form of Tim23 are underlined in red. The PK-cleavage site is indicated with a down-arrow. (b) WT mitochondria were energized in the presence of NADH, ATP and ATP-regenerating system or incubated in the presence of valinomycin and oligomycin to dissipate membrane potential before PK was added. After 2, 10, 20, and 40 min, samples were taken out, and protease was inhibited. Samples were analyzed by SDS-PAGE and immunoblotting. Tom70 and Tim50 were used as markers for outer and inner membrane proteins, respectively. *Full-length and **clipped versions of Tim23.

extends all the way to the cytosolic surface of mitochondria, making Tim23 the only so far known protein that spans two membranes. We determined that the externally added protease cuts Tim23 after residue 17. Whether Tim23 crosses the outer membrane once or as a loop remains unfortunately unclear. It is also unclear whether Tim23 reaches the cytosolic surface of mitochondria through the lipid bilayer or through a proteinaceous channel in the outer membrane. If latter, the TOM complex would be a feasible candidate. What is clear is that this two-membrane topology of Tim23 brings the two mitochondrial membranes, and thus also TOM and TIM23 complexes, closer together, facilitating translocation of proteins along the presequence pathway.

Our analysis revealed several events in the IMS that extend their influence across membranes. First, we demonstrated an unanticipated direct interaction of Tim23 with Pam17 in the IMS. The effects of Tim23–Pam17 interaction in the IMS are sensed in the matrix, where the two proteins were previously shown to interact. On the other hand, the effects of mutations in the very end of the IMS-exposed domain of Tim23, very close to the inner membrane, extend to the cytosolic surface of mitochondria – the

95 K2 mutation impaired formation of crosslinked Tim23 dimers and, at the same time, made Tim23 more readily exposed on the mitochondrial surface. Another phenomenon that extends its influence from the inner to the outer membrane through Tim23 is membrane potential. We observed that dissipation of the membrane potential across the inner membrane reduced the exposure of Tim23 on the mitochondrial surface. Previous work demonstrated an active role of membrane potential in determining the conformation of the membrane embedded segments of Tim23 [12,33], suggesting how signals from within mitochondria can be transduced to the surface of the organelle through the IMS domain of Tim23.

Taken together, our results suggest a model in which an intricate network of Tim23 interactions in the IMS transduces its influence across two mitochondrial membranes, ensuring coordinated and efficient translocation of proteins from the cytosol into the mitochondrial matrix.

Materials and Methods

Strains, plasmids, and growth conditions

Tim23 shuffling strain in YPH499 yeast background [28] was used to generate all yeast mutants. Tim23 N-terminal truncation mutants and alanine scanning mutants were made in centromeric yeast vectors pRS315 and pRS314, respectively, using standard molecular biology techniques. All constructs were expressed under the control of endogenous *TIM23* promoter and 3'UTR. p415GPD plasmid was used for overexpression of Tim23 Δ 30. The same plasmid was also used to generate C-terminally His-tagged Tim23 variants with *amber* Stop codon for incorporation of Bpa at specified positions. Incorporation of Bpa at the *amber* Stop codon-defined positions was made possible by co-transformation of yeast cells with the plasmid pBpa2-PGK1 + 3SUP4-tRNA_{CUA} [40], which encodes for the respective tRNAs and aminoacyl-tRNA synthetase. In all cases, the WT copy of Tim23, encoded on the *URA*-plasmid in the Tim23 shuffling strain, was chased out on the medium containing 5-fluoroorotic acid.

For drop dilution spot assay, yeast cells were grown in YPD medium prior to spotting on YPD or YPLac plates. Mitochondria were isolated from cells grown at 24 °C in lactate medium containing 0.1% glucose. For *in vivo* site-specific crosslinking, yeast cells were grown in selective glucose medium supplemented with required markers and 1 mM Bpa.

Multiple sequence alignment

Seven hundred ninety-five Tim23 sequences from different species [35] were aligned using Clustal

Omega [41], and the resulting multiple sequence alignment was converted to WebLogo chart using Weblogo creation tool at weblogo.berkeley.edu/logo.cgi [42]. The segments absent in the IMS domain of yeast Tim23 were excluded from the analysis.

Membrane potential measurements

Membrane potential sensitive dye DiSC₃(5) (500 nM) was added to 1.5 ml of SI buffer (50 mM Hepes-KOH, 0.6 M sorbitol, 75 mM KCl, 10 mM Mg (Ac)₂, 2 mM KH₂PO₄, 2.5 mM EDTA, 2.5 mM MnCl₂, 2 mM NADH (pH 7.2)) and the fluorescent signal measured in real time (excitation, 622 nm; emission, 670 nm). Isolated mitochondria (20 µg) and valinomycin (2 µM) were added to the reaction at indicated time points.

In vivo site-specific crosslinking

Yeast cells expressing versions of Tim23 with Bpa at indicated positions were harvested by centrifugation and resuspended in 10 ml of ice-cold SD medium. One-half was exposed to UV light (365 nm, 100 W, 230 V) on ice for 1 h, while the other half was kept in dark. Total cell extracts were prepared [43] and analyzed by SDS-PAGE and immunoblotting.

For enrichment of His-tagged Tim23 and its crosslinking products, total cell extracts were diluted 1:10 with 50 mM Tris, 300 mM NaCl, 0.5% (v/v) triton X-100, 20 mM imidazole, 1 mM PMSF (pH 8.0) and incubated with NiNTA-Agarose beads at 4 °C for 30 min on an overhead shaker. Specifically bound proteins were eluted with Laemmli buffer containing 300 mM imidazole and analyzed by SDS-PAGE and immunoblotting.

Miscellaneous

Previously described methods were used for drop dilution spot assay [44], chemical crosslinking in intact mitochondria [45], coimmunoprecipitation [44], *in vitro* crosslinking with purified proteins [28,36], protein import into isolated mitochondria [22], and proteinase K treatment of intact mitochondria [31].

CRedit authorship contribution statement

Umut Günsel: Conceptualization, Investigation, Validation, Visualization, Writing - original draft, Writing - review & editing. **Eyal Paz:** Investigation, Validation, Visualization, Writing - review & editing. **Ruhita Gupta:** Investigation, Writing - review & editing. **Isabella Mathes:** Investigation, Writing - review & editing. **Abdussalam Azem:** Validation, Writing - review & editing, Supervision, Funding acquisition. **Dejana Mokranjac:** Conceptualization,

Investigation, Validation, Visualization, Writing - original draft, Writing - review & editing, Supervision, Funding acquisition.

Acknowledgments

We thank Petra Robisch and Zdenka Stanic for their expert technical assistance; Drs Kai Hell and Christof Osman for careful reading and comments on the manuscript; Dr. Peter Schultz, the Scripps Research Institute, for providing the pBpa2-PGK1 + 3SUP4-tRNA_{CUA} plasmid; Dr. Toshiya Endo, Kyoto Sangyo University, for an antibody against Tim21; and Dr. Friedrich Lottspeich, MPI of Biochemistry, for his support during Edman degradation experiment. We gratefully acknowledge the generous financial support from Deutsche Forschungsgemeinschaft (MO1944/1-1 and MO1944/1-2 to D.M.), Joint Research Projects on Biophysics LMU-TAU (to D.M. and A.A.), Friedrich-Baur Stiftung (to D.M.), and Israel Science Foundation (1389/18 to A.A.).

Declaration of Competing Interest

The authors declare no conflict of interest.

Appendix A. Supplementary data

Supplementary data to this article can be found online at <https://doi.org/10.1016/j.jmb.2020.03.031>.

Received 17 December 2019;
Received in revised form 5 March 2020;
Accepted 31 March 2020
Available online 8 April 2020

Keywords:
mitochondria;
protein sorting;
protein translocation;
TIM23 complex;
presequence pathway

Abbreviations used:
IMS, intermembrane space; WT, wild-type; Bpa, p-benzoyl-phenylalanine.

References

- [1] P.E. Wright, H.J. Dyson, Intrinsically disordered proteins in cellular signalling and regulation, *Nat Rev Mol Cell Biol* 16 (2015) 18–29.

- [2] T. Endo, K. Yamano, S. Kawano, Structural insight into the mitochondrial protein import system, *Biochim. Biophys. Acta* 1808 (2011) 955–970.
- [3] U. Günsel, D. Mokranjac, A journey along the TIM23 complex, the major protein translocase of the mitochondrial inner membrane, *Biologia Serbica* 41 (2019) 27–35.
- [4] K.G. Hansen, J.M. Herrmann, Transport of proteins into mitochondria, *Protein J.* 38 (2019) 330–342.
- [5] W. Neupert, A perspective on transport of proteins into mitochondria: a myriad of open questions, *J. Mol. Biol.* 427 (2015) 1135–1158.
- [6] C. Schulz, A. Schendzielorz, P. Rehling, Unlocking the presequence import pathway, *Trends Cell Biol.* 25 (2015) 265–275.
- [7] N. Wiedemann, N. Pfanner, Mitochondrial machineries for protein import and assembly, *Annu. Rev. Biochem.* 86 (2017) 685–714.
- [8] M. Wasilewski, K. Chojnacka, A. Chacinska, Protein trafficking at the crossroads to mitochondria, *Biochim Biophys Acta Mol Cell Res* 1864 (2017) 125–137.
- [9] Y. Kang, L.F. Fielden, D. Stojanovski, Mitochondrial protein transport in health and disease, *Semin. Cell Dev. Biol.* 76 (2018) 142–153.
- [10] N.N. Alder, R.E. Jensen, A.E. Johnson, Fluorescence mapping of mitochondrial TIM23 complex reveals a water-facing, substrate-interacting helix surface, *Cell* 134 (2008) 439–450.
- [11] N. Denkert, A.B. Schendzielorz, M. Barbot, L. Versemann, F. Richter, P. Rehling, M. Meinecke, Cation selectivity of the presequence translocase channel Tim23 is crucial for efficient protein import, *Elife* 6 (2017), e28324.
- [12] K. Malhotra, M. Sathappa, J.S. Landin, A.E. Johnson, N.N. Alder, Structural changes in the mitochondrial Tim23 channel are coupled to the proton-motive force, *Nat. Struct. Mol. Biol.* 20 (2013) 965–972.
- [13] S. Martinez-Caballero, S.M. Grigoriev, J.M. Herrmann, M.L. Campo, K.W. Kinnally, Tim17p regulates the twin pore structure and voltage gating of the mitochondrial protein import complex TIM23, *J. Biol. Chem.* 282 (2007) 3584–3593.
- [14] A. Ramesh, V. Peleh, S. Martinez-Caballero, F. Wollweber, F. Sommer, M. van der Laan, M. Schroda, R.T. Alexander, et al., A disulfide bond in the TIM23 complex is crucial for voltage gating and mitochondrial protein import, *J. Cell Biol.* 214 (2016) 417–431.
- [15] K.N. Truscott, P. Kovermann, A. Geissler, A. Merlin, M. Meijer, A.J. Driessen, J. Rassow, N. Pfanner, et al., A presequence- and voltage-sensitive channel of the mitochondrial preprotein translocase formed by Tim23, *Nat. Struct. Biol.* 8 (2001) 1074–1082.
- [16] L. Wrobel, A.M. Sokol, M. Chojnacka, A. Chacinska, The presence of disulfide bonds reveals an evolutionarily conserved mechanism involved in mitochondrial protein translocase assembly, *Sci. Rep.* 6 (2016) 27484.
- [17] M.F. Bauer, C. Sirrenberg, W. Neupert, M. Brunner, Role of Tim23 as voltage sensor and presequence receptor in protein import into mitochondria, *Cell* 87 (1996) 33–41.
- [18] A. Chacinska, P. Rehling, B. Guiard, A.E. Frazier, A. Schulze-Specking, N. Pfanner, W. Voos, C. Meisinger, Mitochondrial translocation contact sites: separation of dynamic and stabilizing elements in formation of a TOM–TIM–preprotein supercomplex, *EMBO J.* 22 (2003) 5370–5381.
- [19] A. Geissler, A. Chacinska, K.N. Truscott, N. Wiedemann, K. Brandner, A. Sickmann, H.E. Meyer, C. Meisinger, et al., The mitochondrial presequence translocase: an essential role of Tim50 in directing preproteins to the import channel, *Cell* 111 (2002) 507–518.
- [20] O. Lytovchenko, J. Melin, C. Schulz, M. Kilisch, D.P. Hutu, P. Rehling, Signal recognition initiates reorganization of the presequence translocase during protein import, *EMBO J.* 32 (2013) 886–898.
- [21] K. Malhotra, A. Modak, S. Nangia, T.H. Daman, U. Günsel, V. L. Robinson, D. Mokranjac, E.R. May, et al., Cardiolipin mediates membrane and channel interactions of the mitochondrial TIM23 protein import complex receptor Tim50, *Sci. Adv.* 3 (2017), e1700532.
- [22] D. Mokranjac, S.A. Paschen, C. Kozany, H. Prokisch, S.C. Hoppins, F.E. Nargang, W. Neupert, K. Hell, Tim50, a novel component of the TIM23 preprotein translocase of mitochondria, *EMBO J.* 22 (2003) 816–825.
- [23] D. Mokranjac, M. Sichtung, D. Popov-Celeketic, K. Mapa, L. Gevorkyan-Airapetov, K. Zohary, K. Hell, A. Azem, et al., Role of Tim50 in the transfer of precursor proteins from the outer to the inner membrane of mitochondria, *Mol. Biol. Cell* 20 (2009) 1400–1407.
- [24] C. Schulz, O. Lytovchenko, J. Melin, A. Chacinska, B. Guiard, P. Neumann, R. Ficner, O. Jahn, et al., Tim50's presequence receptor domain is essential for signal driven transport across the TIM23 complex, *J. Cell Biol.* 195 (2011) 643–656.
- [25] Y. Tamura, Y. Harada, T. Shiota, K. Yamano, K. Watanabe, M. Yokota, H. Yamamoto, H. Sesaki, et al., Tim23–Tim50 pair coordinates functions of translocators and motor proteins in mitochondrial protein import, *J. Cell Biol.* 184 (2009) 129–141.
- [26] H. Yamamoto, M. Esaki, T. Kanamori, Y. Tamura, S. Nishikawa, T. Endo, Tim50 is a subunit of the TIM23 complex that links protein translocation across the outer and inner mitochondrial membranes, *Cell* 111 (2002) 519–528.
- [27] D. Dayan, M. Bandel, U. Günsel, I. Nussbaum, G. Prag, D. Mokranjac, W. Neupert, A. Azem, A mutagenesis analysis of Tim50, the major receptor of the TIM23 complex, identifies regions that affect its interaction with Tim23, *Sci. Rep.* 9 (2019) 2012.
- [28] L. Gevorkyan-Airapetov, K. Zohary, D. Popov-Celeketic, K. Mapa, K. Hell, W. Neupert, A. Azem, D. Mokranjac, Interaction of Tim23 with Tim50 is essential for protein translocation by the mitochondrial TIM23 complex, *J. Biol. Chem.* 284 (2009) 4865–4872.
- [29] M. Donzeau, K. Kaldi, A. Adam, S. Paschen, G. Wanner, B. Guiard, M.F. Bauer, W. Neupert, et al., Tim23 links the inner and outer mitochondrial membranes, *Cell* 101 (2000) 401–412.
- [30] D. Popov-Celeketic, K. Mapa, W. Neupert, D. Mokranjac, Active remodelling of the TIM23 complex during translocation of preproteins into mitochondria, *EMBO J.* 27 (2008) 1469–1480.
- [31] K. Waagemann, D. Popov-Celeketic, W. Neupert, A. Azem, D. Mokranjac, Cooperation of TOM and TIM23 complexes during translocation of proteins into mitochondria, *J. Mol. Biol.* 427 (2015) 1075–1084.
- [32] R. Bajaj, L. Jaremko, M. Jaremko, S. Becker, M. Zweckstetter, Molecular basis of the dynamic structure of the TIM23 complex in the mitochondrial intermembrane space, *Structure* 22 (2014) 1501–1511.
- [33] N.N. Alder, J. Sutherland, A.I. Buhring, R.E. Jensen, A.E. Johnson, Quaternary structure of the mitochondrial TIM23 complex reveals dynamic association between Tim23p and other subunits, *Mol. Biol. Cell* 19 (2008) 159–170.

- [34] L. de la Cruz, R. Bajaj, S. Becker, M. Zweckstetter, The intermembrane space domain of Tim23 is intrinsically disordered with a distinct binding region for presequences, *Protein Sci.* 19 (2010) 2045–2054.
- [35] V. Zarsky, P. Dolezal, Evolution of the Tim17 protein family, *Biol. Direct* 11 (2016) 54.
- [36] M. Marom, D. Dayan, K. Demishtein-Zohary, D. Mokranjac, W. Neupert, A. Azem, Direct interaction of mitochondrial targeting presequences with purified components of the TIM23 protein complex, *J. Biol. Chem.* 286 (2011) 43809–43815.
- [37] A.B. Schendzielorz, C. Schulz, O. Lytovchenko, A. Clancy, B. Guiard, R. Ieva, M. van der Laan, P. Rehling, Two distinct membrane potential-dependent steps drive mitochondrial matrix protein translocation, *J. Cell Biol.* 216 (2017) 83–92.
- [38] M. van der Laan, A. Chacinska, M. Lind, I. Perschil, A. Sickmann, H.E. Meyer, B. Guiard, C. Meisinger, et al., Pam17 is required for architecture and translocation activity of the mitochondrial protein import motor, *Mol. Cell. Biol.* 25 (2005) 7449–7458.
- [39] A. Chacinska, M. Lind, A.E. Frazier, J. Dudek, C. Meisinger, A. Geissler, A. Sickmann, H.E. Meyer, et al., Mitochondrial presequence translocase: switching between TOM tethering and motor recruitment involves Tim21 and Tim17, *Cell* 120 (2005) 817–829.
- [40] S. Chen, P.G. Schultz, A. Brock, An improved system for the generation and analysis of mutant proteins containing unnatural amino acids in *Saccharomyces cerevisiae*, *J. Mol. Biol.* 371 (2007) 112–122.
- [41] F. Madeira, Y.M. Park, J. Lee, N. Buso, T. Gur, N. Madhusoodanan, P. Basutkar, A.R.N. Tivey, et al., The EMBL-EBI search and sequence analysis tools APIs in 2019, *Nucleic Acids Res.* 47 (2019) W636–W641.
- [42] G.E. Crooks, G. Hon, J.M. Chandonia, S.E. Brenner, WebLogo: a sequence logo generator, *Genome Res.* 14 (2004) 1188–1190.
- [43] V.V. Kushnirov, Rapid and reliable protein extraction from yeast, *Yeast* 16 (2000) 857–860.
- [44] K. Demishtein-Zohary, U. Gunsel, M. Marom, R. Banerjee, W. Neupert, A. Azem, D. Mokranjac, Role of Tim17 in coupling the import motor to the translocation channel of the mitochondrial presequence translocase, *Elife* 6 (2017), e22696.
- [45] R. Banerjee, U. Gunsel, D. Mokranjac, Chemical crosslinking in intact mitochondria, *Methods Mol. Biol.* 1567 (2017) 139–154.